J. Cell. Mol. Med. Vol 13, No 10, 2009 pp. 4166-4175

Regression and persistence: remodelling in a tissue engineered axial vascular assembly

E. Polykandriotis [a, *], S. Euler [b], A. Arkudas [a], G. Pryymachuk [a], J. P. Beier [a], P. Greil [c], A. Dragu [a], A. Lametschwandtner [d], U. Kneser [a], R. E. Horch [a]

[a] Department of Plastic and Hand Surgery, University of Erlangen, Erlangen, Germany
[b] Department of Trauma Surgery and Sports Medicine, University of Innsbruck, Innsbruck, Austria
[c] Institute of Materials Science, Glass and Ceramics, University of Erlangen, Erlangen, Germany
[d] Department of Organismic Biology, University of Salzburg, Salzburg, Austria

Received: April 17, 2009; Accepted: June 10, 2009

Abstract

In later stages of vasculoangiogenesis a vascular network is going through a metamorphosis for optimal perfusion and economy of energy. In this study we make a quantitative approach to phenomena of remodelling in a bioartificial neovascular network and suggest variance of calibre as a parameter of neovascular maturation. For this study, 18 male Lewis rats were subjected to the AV loop operation in combination with a hard porous biogenic matrix and an isolation chamber. The animals were allocated into three groups for different explantation intervals set to 2, 4 and 8 weeks, respectively. Collective attributes like vascular density, percent fractional area and variance of calibre were evaluated for a predefined region of interest (ROI). Late morphogenesis was evaluated by means of scanning electron microscopy. After the fourth week the absolute number of vessels within the ROI decreased ($P < 0.03$) whereas, on the contrary, the fractional area of all segments increased ($P < 0.02$). The variance in calibre was significantly increased in the 8-week group ($P < 0.05$). Lymphatic growth after week 4, early pericyte migration as well as intussusceptive angiogenesis were identified immunohistologically. Phenomena of remodelling were evaluated quantitatively in a neovascular network and variance could be proposed as a parameter of net vascular maturation.

Keywords: angiogenesis • remodelling • arteriovenous loop • tissue engineering • vascular regression

Introduction

Angiogenesis has been the subject of extensive research for over 30 years [1, 2]. Especially, antiangiogenesis as a therapeutic strategy against cancer is currently in focus after the first line of antiangiogenic drugs cleared FDA approval [3, 4]. On the other hand, a bright new field of research zeroing onto translational technologies has emerged in a time when tissue engineering meets the challenge of clinical application [5, 6]; a change of paradigmata was necessary to cope with the issues of biocompatibility, upscaling and bioassimilation of bioengineered constructs [7, 8]. In this 'post-tissue-engineering' era, matters of vasculoangiogenesis play a cardinal role, and issues of vascular arborisation as well as maturation and remodelling are subject of ongoing research [8–10]. Evidence of vascular maturation includes presence of perivascular cellular elements, formation of a capillary loop and regression of capillary surplus with persistence and remodelling of the remaining vessels. It is important to emphasize that understanding of these processes both in the molecular as well as the mophologic level is necessary because 'the inherent design principles are not encoded by genes alone, but emerge from a complex interaction of haemodynamic forces and epigenetic processes coupled to those forces' [11].

The presence of perivascular cellular elements like smooth muscle cells (SMC) and pericytes (PCT) are indicators of maturity for a single vascular conduit. It has been suggested that the angiopoietin class of molecules plays an important role in this process of perivascular cell adhesion contributing to vessel integrity [12]. However, new data indicate that the roles of the endothelial cells (EC) and the PCTs in respect to the first stages of

*Correspondence to: Elias POLYKANDRIOTIS, M.D.
Department of Plastic and Hand Surgery,
University of Erlangen, Krankenhausstrasse 12,
91054 Erlangen, Germany.
Tel.: +49-9131-85-33277
Fax: +49-9131-85-39327
E-mail: elias.polykandriotis@uk-erlangen.de

doi:10.1111/j.1582-4934.2009.00828.x

endothelial proliferation and migration might be interchangeable; PCT could after all be the first to proliferate and form a perivascular outsprout into the proangiogenic interstitium only to be followed by endothelial proliferation [13]. That would in turn disqualify PCT as indicators of maturation of nascent vessels.

The mechanisms behind formation of an arteriovenous capillary loop by means of interconnection of pre-existing neovascular conduits are not entirely understood. It has been suggested that pericytic processes bridging the gap between the leading edges of opposing endothelial sprouts, may serve as guiding structures for the outgrowth of EC [14]. Recently, the Eph family of receptors has been shown to be involved in specifying the fate of EC destined to localize in either the arterial or venous side of the circulation [15, 16]. Current data are highly suggestive that the EphB class of molecules acquire a key role in orchestrating anastomosis at the capillary–capillary junction [17]. However, interconnection of nascent capillaries to form a closed arteriovenous circuit is not the only process involved. Another phenomenon seen in formation of an arteriovenous loop, is intussusceptive arborisation (IAR), a term coined to describe separation of the arterial and venous vascular system through formation of interstitial pillars [18].

Intussusception and pruning are both involved in the process of vascular regression. Downregulation of VEGF leads to involution of newly formed capillaries, but other mechanisms might be involved as well. Involution is an integral part of advanced angiogenesis and some vessels have to regress in favour of others, which persist and eventually form vessels of a greater calibre [18]. Two distinct processes of regression have been suggested: vascular occlusion and pruning. In the first, the leading event is aggregation of platelets, stasis of blood and degeneration of vessel walls, probably as a result of sluggish blood flow. Alternatively, in pruning, the process is characterized by protrusion of endothelial cells into the lumen, and formation of adherence junctions to other mural ECs [19]. The molecular biology behind intussusception remains to be deciphered.

Finally, enlargement of persisting capillaries into arterioles and venules, by way of arteriogenesis, is most probably promoted by monocytes [19]. At the far end of the process of persistence and regression stands an optimally perfusing architecture with a hierarchical organisation of the vessels into small arteries, arterioles, precapillary arterioles and gas-exchanging capillaries with a blood flow draining into postcapillary venules and greater veins [20].

In this study we describe phenomena of remodelling in a bioartificial neovascular system and suggest variance of calibre as a parameter of vascular bed maturation, in an attempt to dissect these processes of late morphogenesis in this vascular assembly.

Materials and Methods

Animals and groups

Inbred male Lewis rats weighing approximately 250 g each were used in this study (Charles River, Sulzfeld, Germany). A total of 18 animals were divided in three groups according to the point of explantation after the initial operation. The implantation-to-explantation intervals were set to 2, 4 and 8 weeks with $n = 6$ for each group. One animal from each group was subjected to perfusion with a low viscosity resin for corrosion casting whereas the rest were subjected to India ink perfusion and histological processing. Sample size was adjusted, according to previous studies on the patient [21, 22]. All experiments were approved by the animal care committee of the University of Erlangen and the Government of Mittelfranken (PN:621.2531.32–06/03).

Matrix and tissue isolation chamber

The design of the isolation chamber and the matrix have been described previously [21] (Fig. 1). Briefly, a flat cylindrical Teflon chamber with an aperture for the entering arteriovascular pedicle and a press-fitting cup was constructed by the Institute of Materials Science; Division of Glass and Ceramics, University of Erlangen. The porous matrix (Tutobone, Tutogen Medical, Neunkirchen, Germany) consisted of processed bovine cancellous bone in the form of a disc 9 mm in diameter and 5 mm in height. Around the periphery of the disc there was a 1.5 × 2 mm groove accommodating the arteriovenous loop.

Surgical procedures

All implantation procedures took place under general anaesthesia with Isoflurane (Baxter, Unterschleiβheim, Germany). Prior to surgery the rats were given an injection of a 0.2 ml broad-spectrum antibiotic (Tardomycel Comp III, Bayer, Leverkusen, Germany). The femoral neurovascular bundle was exposed through a 4-cm long incision at the medial thigh. Dissection of the vessels extended from the pelvic artery in the groin to the bifurcation of the popliteal artery in the knee. After dissection of the artery and vein, a femoral venous graft was harvested from the contralateral side and interposed between the femoral vessels by anastomoses using an 11–0 Nylon suture (Ethilon, Ethicon, Norderstedt, Germany). The new vascular construct was an arteriovenous loop (AV loop) (Fig. 1). The isolation chamber with the matrix was placed in the medial thigh of the rat and the AV loop was placed into the peripheral groove around the matrix disc. The anastomosis between vein and graft was marked with a small indentation on the upper side of the disk for later orientation. The lid was closed and the chamber was fixed onto the deep adductor fascia with a non-absorbable Polypropylene suture. Interrupted vertical mattress sutures with Vicryl 4–0 were used for wound closure.

Upon explantation, the aorta and inferior vena cava were exposed through a median incision from the xiphoid process to the pubic symphysis. By means of a 24G catheter the aorta was canulated and the inferior vena cava severed to allow for exsanguination and perfusion with heparinized, saline (200 ml, 80 IU/ml, 37°C). As soon as the fluid from the inferior vena cava was clear, the animal was perfused with 3% Glutaraldehyde (Roth, Karlsruhe, Germany) and then either with a 30 ml mixture of 50% v/v India Ink (Rohrer, Germany), 5% Gelatine (Roth, Karlsruhe, Germany) and 4% Mannitol (Neolab, Heidelberg, Germany) or with 20 ml of a low viscosity resin (Mercox II, Ladd Research Industries, Burlington, VT, USA).

Histology and morphometric analysis

Kinetics of vascularization in this matrix were described before [21]. In this study we concentrated on remodelling phenomena within the

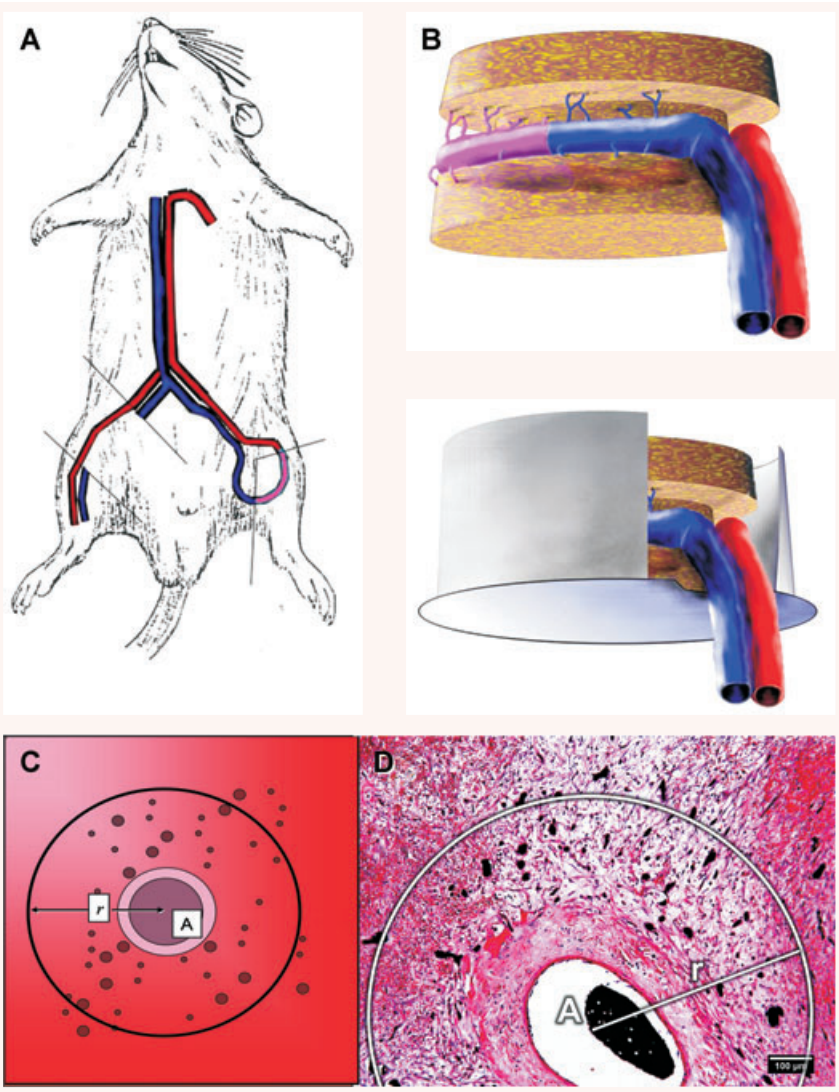

Fig. 1 (**A**) For construction of the AV loop, a segment of the right femoral vein is being harvested and interposed between the left femoral artery and vein. (**B**) The AV loop is placed in the peripheral groove of the porous matrix. Neovascular sprouts enter the matrix and render it vascularized. The construct is placed into an isolation chamber with an aperture for entrance of the vascular pedicle of the AV loop. (**C**) Method of analysis: A ROI was defined in a 500 μm radius (r) around the vascular axis (A), excluding the loop vessel itself. The image was rendered bimodal with a standardized threshold set to black stained India ink-filled vessels. The bimodal images were detected and analyzed for % FA of vessels against ROI (% FA), absolute capillary number (CapNo) in ROI as well as differential vascular calibre in ROI. In this way a developing vascular segment rather than an expanding one was evaluated. (**D**) Example on an acquired image.

previously defined ROI. The vascular lumina were visualized as black areas by the India ink gel injection. Shrinkage of the India ink of various degrees could be seen in the vascular lumina of greater calibre. These elements had to be manually corrected prior to histomorphometrical analysis.

All tissues were explanted *in toto* in a standardized fashion and subjected to decalcification with EDTA. After fixation in 3.7% neutral buffered formalin the decalcified matrix was divided on a central plane perpendicular to the disc into a distal and a proximal part. Five micrometer histological sections were obtained with a Leica microtome (Leica Microsystems, Bensheim, Germany) from each semidisc from one standardized plane 2 mm from the central plane, or another 1 mm from the graft-vein anastomosis when necessary. In this way, cross sections of all artery, vein and graft segments could be obtained for evaluation. The sections were prepared by standard methods and stained with haematoxylin and eosin. Microphotographs were taken using a Leica microscope and digital camera. Digital processing of the original pictures was only performed for the purpose of morphometric analysis (ImageJ, W. Rasband, National Institutes of Health, Bethesda, MD, USA) Images were acquired from the region of the vascular axis under 100× magnification. By means of a semi-automated algorithm, a region of interest (ROI) was defined in a 500 μm circumference around the vascular axis, excluding the loop vessel itself. The image was rendered bimodal with a standardized threshold set to black stained India ink-filled vessels. The bimodal images were detected and analyzed for per cent fractional area (% FA) of vessels against ROI (% FA), absolute capillary number (CapNo) in ROI as well as differential vascular calibre (variance of calibre) in ROI. The measurements were performed by two blinded observers (Fig. 2).

For statistical analysis, % FA, CapNo and variance of vascular calibre were tested positive for normal distribution and suitable for parametric tests (Kolmogorov–Smirnov test). Variance of vascular calibre was calculated for all segments of the loop. One-way analysis of variance

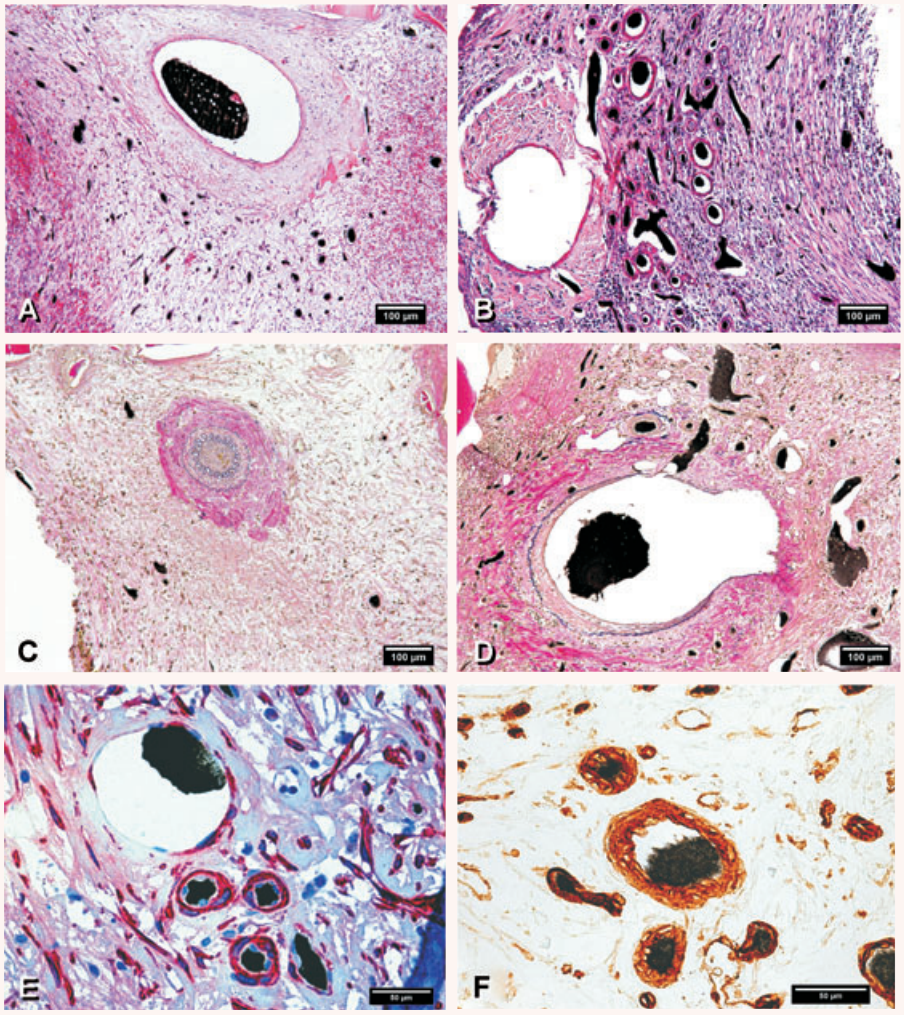

Fig. 2 (**A**) Venous segment, 2 weeks: The vascular network consists of numerous but small vessels, characteristic for an expanding neovascular system. The vascular axis filled with India ink gel is seen in the middle (HE, ×100). (**B**) Venous segment, 8 weeks: The number of vessels is not significantly higher but the calibre varies greatly building a vascular hierarchy from arterioles and precapillary arterioles, to gas-exchanging capillaries, postcapillary venules and venules draining into veins (HE, ×100). (**C**) Arterial segment, 4 weeks. Around the artery the neovascularization is sparse. The artery possesses a distinct tunica elastica and a thick muscular layer (van Gieson-Verhoeff, ×100). (**D**) Identical specimen as in 2c, venous segment. A marked difference from the arterial segment can be observed in terms of luminal calibre, variance and number. The vein shows some intimal hyperplasia concomitant with the arterialization process after construction of the AV loop. (van Gieson-Verhoeff, ×100). (**E**) Venous segment, 4 weeks. PCT stain red, endothelial cells and polymorphonuclear cells stain blue. PCT provide stabilization of the endothelium-their presence is thought to be a sign of maturation in a vessel (α-SM actin, ×250). (**F**) Lectin staining of endothelial cells demonstrates functionally full-grown vessels. On the upper right corner of the image there are three vascular conduits positive for lectin but void of India ink. Such a finding might be indicative of lympnatics present as soon as 4 weeks after initiation of neovascularization (lectin, ×350).

(ANOVA) with Bonferroni adjustment for multiple comparisons was used for these parameters. Significance was set to $P < 0.05$ for all measurements. Standard error of the means was used for graphic display of the results.

Further sections were processed for double (van Gieson-Verhoeff) collagen–elastin staining and immunohistology with α-smooth muscle actin (α-SMA) and lectin. For lectin, (Griffonia simplicifolia-1) 1:270, biotinylated lectin-Gs-1 (Sigma Aldrich, Munich, Germany) followed by peroxidase-conjugated streptavidin (DakoCytomation, Hamburg, Germany) and exposed to 3,3 diaminobenzidine (DAB) substrate was used. For α-SMA, a staining kit (1:300 Zytomed, Berlin, Germany) was used according to the manufacturer's protocol. Sections were deparaffinated and incubated overnight at 4°C with 1:300 mouse anti-ASMA primary antibody (Dako GmbH, Germany). An anti-mouse anti-rabbit

secondary antibody (Invitrogen, Carlsbad, CA, USA) was used for 30 min. at room temperature. The enzyme was revealed with 0.2 mg/ml naphthol AS.MX (Sigma Chemical Co, St. Louis, MO, USA), 0.002 mg/ml dimethyl formamide (Merck, Darmstadt, Germany) in 0.1 M Tris pH 8,2, 1 mg/ml fast red TR salt (Sigma Chemical Co), and 0.33 mg/ml Levamisole (Sigma Chemical Co). Sections were counterstained with hematoxylin (Merck).

Corrosion cast technique

The technique of perfusion and maceration has been described previously [23]. The vascular replicas were mounted on probe plates and rendered conductive by means of copper bridging [24] and gold sputtering. Images of the specimens were obtained on a Cambridge Stereoscan 250 MKII device (Cambridge Instrument Co. Ltd., Cambridge, UK).

Results

Surgery, vascular patency

Overall patency rate was approximately 85%. Thrombosed constructs were excluded from further evaluation and the experiment was repeated until $n = 6$ was completed for each group.

Histology: morphological observations

As confirmed by histomophometry in the 2-week group the vascular lumina seemed uniformly small, with a diameter ranging from 7 to 15 micrometers (μm) (Fig. 2A). In the 4-week group the number of lumina increased but it was not until week 8 that the nascent capillaries displayed the pattern of a highly variable neovascular network, with large vessels alternating with small capillaries with calibre size ranging from 10 to 100 μm (Fig. 2B).

Verhoeff–van Gieson staining displayed the characteristic cross-sectional structure of the artery and arterialized vein as constituents of the AV loop while the graft segment displayed some degree of neointimal hyperplasia (Fig. 2C and D). Angiogenic activity in the vicinity of the artery was clearly delayed both in terms of quantity and quality. These findings would confirm anew the venous side of the circulation as the primary source of neovascularization [19].

α-SMA positive PCT were present at all vascular conduits indicating migration of PCTs as soon as 2 weeks after initiation of angiogenesis (Fig. 2E). India Ink free lumina appeared in the 4- and 8-week specimens probably indicating presence of lymphatics. (Fig. 2F). On the contrary, there were indeed lumina positive for lectin, identifying them as vessels and positive for α-SMA without any visible lumen. This might indicate that pericyte migration takes place before or concomitantly to formation of a neovascular lumen (Fig. 3A and B).

Finally, dividing vessels were also identified, maybe indicative of intussusceptive vascular growth (IVG). The dividing pillars were of endothelial origin, rather than fibroblastic. Tangential section of the vascular wall could not be excluded here (Fig. 3C and D).

Morphometric analysis

There was a distinct difference in terms of neovascularization kinetics and remodelling between the arterial and non-arterial segments of the loop. Mean values with standard error of the means (SE) are given here. The percentage of area occupied by vessels *versus* total detected area (% FA of vessels *versus* total ROI) developed as follows: Arterial segment 2 weeks: 0.89 (SE 0.194), 4 weeks: 1.44 (SE 0.124) and 8 weeks: 3.12 (SE 0.737). Venous segment 2 weeks: 3.36 (SE 0.67), 4 weeks: 3.62 (SE 0.293), 8 weeks: 4.87 (SE 1.165). Graft segment 2 weeks: 1.66 (SE 0.349), 4 weeks: 2.59 (SE 0.382), 8 weeks: 4.29 (SE 0.549). There was a significant increase from week 2 to week 8 in all segments ($P < 0.02$).

The absolute number of vascular lumina (CapNo) in the detected area developed as follows: Arterial segment 2 weeks: 52 (SE 6.06), 4 weeks: 148 (SE 15.62), 8 weeks: 217 (SE 82.8). Venous segment 2 weeks: 778 (SE 126), 4 weeks: 1449 (SE 128), 8 weeks: 776 (SE 23). Graft segment 2 weeks: 177 (SE 36.88), 4 weeks: 879 (SE 63.37) and 8 weeks: 442 (SE 120.86). The number of vessels within this ROI increased significantly from week 2 to week 4 in all segments: artery—$P < 0.01$; vein—$P < 0.02$; graft—$P < 0.01$. In the artery there was a continuous increase in the number of lumina throughout the experiment ($P < 0.03$). However, the number of capillary cross sections detected, decreased significantly between week 4 and week 8 in the venous ($P < 0.01$) and graft ($P < 0.03$) segments. The number of vessels in the venous segment was significantly superior to both the arterial ($P < 0.01$) and graft ($P < 0.01$) segments both in the 2-week and the 4-week groups. In the 8-week groups there was no significant difference in the number of lumina between the different segments (A–V: $P = 0.42$; A–G: $P = 1.00$; V–G: $P = 0.36$).

The variance of calibre of vascular lumina detected in the ROI at all segments was as follows: 2 weeks: 215.143×10^3 (SE 88.317×10^3), 4 weeks: 105.619×10^3 (SEM 31.108×10^3), 8 weeks: 643.455×10^3 (SEM 186.243×10^3). The variance in calibre increased significantly between weeks 2 and 8 ($P < 0.05$) as well as between weeks 4 and 8 ($P < 0.01$). Change of variance between weeks 2 and 4 was not significant ($P = 0.18$). The results are summarized in Figs 4 and 5.

Corrosion casts: morphological observations

Phenomena of proliferation and remodelling were found synchronously in all vascular replicas. Neovascular sprouts (Fig. 6B) were clearly more abundant in the 2-week specimen. Clusters of sprouting 'spikes' were found at 'hot spots' of angiogenesis (Fig. 6B). Other regions were quiescent. Near 'hot' regions, but not exactly within them, intussusceptive microvascular growth (IMG) was demonstrated (Fig. 3D).

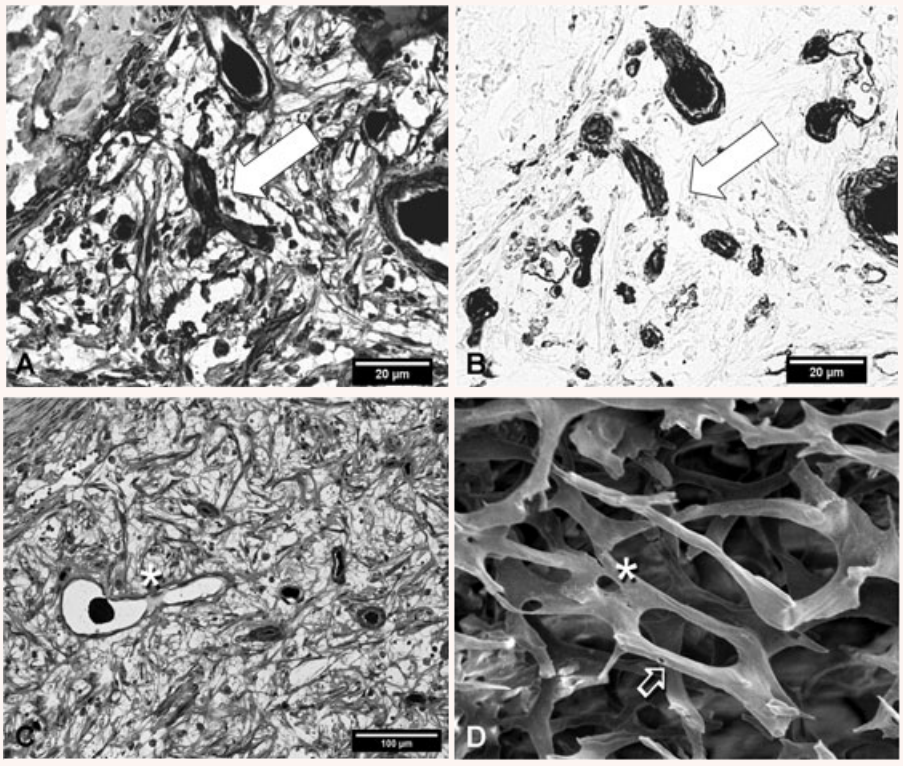

Fig. 3 (**A**) and (**B**) Serial sections of a 2-week specimen. (**A**) In the middle of the image, a neovascular 'tripode' (arrow) with PCT (red staining) encircling the endothelial formation (blue staining of nuclei) shows no India ink filling. On the right side (**B**) the formation shows clearly endothelial staining positive for lectin, with still no India ink filling. This finding is indicative of a vessel furnished with PCT prior to formation of its lumen. Because lumen formation is a relatively early phenomenon of angiogenesis, it seems like pericytic migration and endothelial proliferation are parallel mechanisms, as postulated recently (see text). 4a: α-SM actin, ×350; 4b: lectin; serial sections. (**C**) and (**D**) Non-sprouting angiogenesis by means of intussusceptive microvascular growth (IMG) is an efficient modus for expansion of a neovascular network. In this process a vessel is divided into two vessels by ingrowth (intussusception) of an interstitial pillar. On the right side (**D**) this process is demonstrated on a microvascular replica under the scanning electron microscope. If these pillars are of endothelial or fibroblastic origin is not fully understood. Asterisk: Early stage; Arrow advanced stage showing formation of a new vascular conduit. On the left side (**C**) a venuole is interrupted by an endothelial bridge at the asterisk. One could assume that intussusception is a phenomenon carried out by the endothelial cells; however, remodelling of angiogenesis is grossly a three-dimensional process and is best demonstrated by three-dimensional methods. 3c: (α-SM actin, ×200); 3d: SEM of corrosion casts, ×230.

Formation of loops, that is, interconnections between capillaries or between capillary and feeding vessels, was evident in the 2- and 4-week specimens. Both capillary loop formation by means of IAR (Fig. 6A) and forward conduit interconnection (Fig. 6D and E) could be identified in the 2- and 4-week specimens.

Intussusceptive branching remodelling (IBR), another variation of vascular intussusception was demonstrated in the 4- and 8-week replicas (Fig. 6F). At these sites, remodelling at the branching points takes place by means of interstitial pillars forming along the feeding arterioles prior to the branching itself. IBR is one of the advanced flow optimization mechanisms.

Dedication of the vessels to the arterial or venous side of the circulation occurred at late stages, after an arterial microcirculation was established. The characteristic patterns of venous or arterial wall imprinted on the corrosion cast, were seen exclusively on the 8-week sample (Fig. 6C).

Discussion

In quest for quantification of vasculoangiogenesis, researchers have developed a plethora of ways to couple proliferation to a certain parameter. Experiments with endothelial cells or their progenitor cells *in vitro* have zeroed on profiles of VEGF expression or total length of generated tubule-like-structures [25]. In hybrid *in vivo–in vitro* experiments (*e.g.* aortic ring model, chorioallantoic

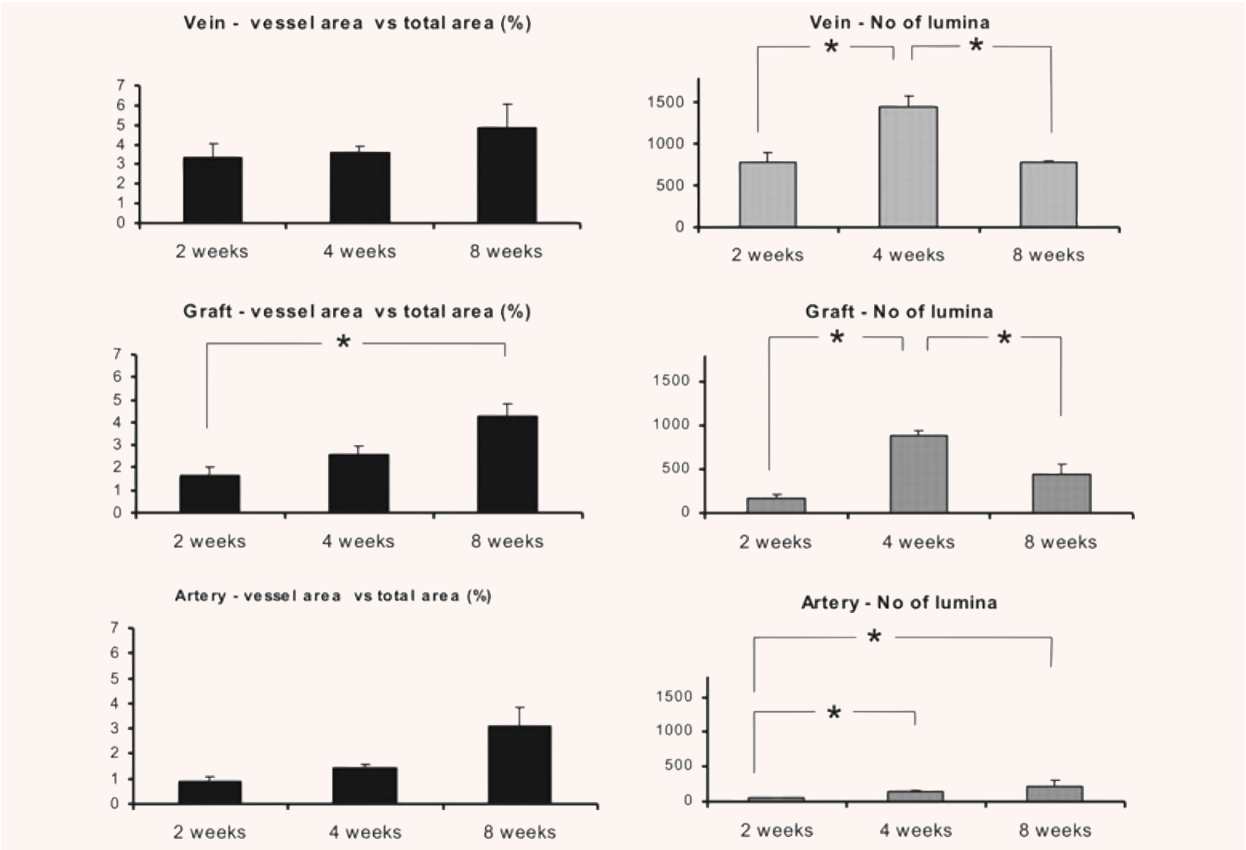

Fig. 4 Left: Cross sectional area of vascular lumina in per cent (% FA) of total area of ROI detected in a radius 500 μm around the vascular axis. Development in all separate segments of the AV loop (vein, graft, artery) over the time intervals 2, 4 and 8 weeks. There is a steady increase over time in all segments indicative of a rise of the summation of the calibre and perfusion volume of all detected vessels. The highest per cent values are met with the vein, demonstrating the highest vasculoangiogenic activity in this region. After 8 weeks values for % FA are comparable all three segments, indicating achievement of a steady state. **Right:** Number of detected vascular lumina within the ROI. Past the 4th week, the number of lumina decreases in the non-arterial segments of the AV loop. Involution of a nascent vascular network in terms of regression of superfluous vessels happens in favour of necessary vascular conduits that persist to form feeding arterioles and draining venules, As angiogenesis in the vicinity of the artery is not as vivid as in the non arterial counterparts, phenomena of remodelling also take place later. For each bar $n = 5$ with 10 independent measurements, (*): $P < 0.05$. Error indicators show standard error of means.

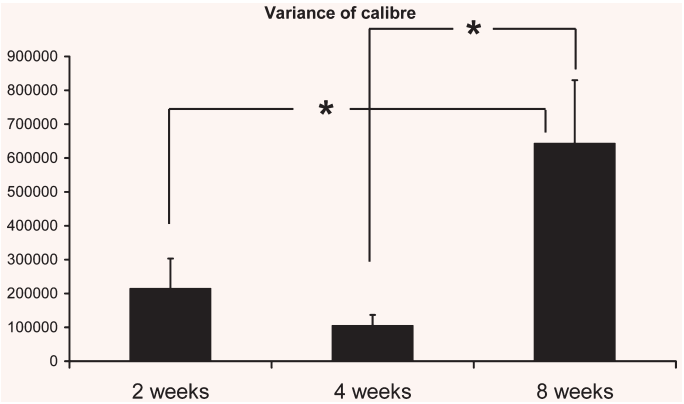

Fig. 5 Luminal diameters (calibre) of individual vessels within a ROI were measured and the variance of calibre was extracted for each ROI. In an attempt to evaluate variance of calibre as a morphologic indicator of maturation for a given neovascular network, this parameter was investigated for all time intervals. The 8-week group presented a significantly higher variance of vascular calibre than either of the 2- and 4-week groups. For each bar $n = 5$, 30 independent measurements, (*): $P < 0.05$. Error indicators show standard error of means.

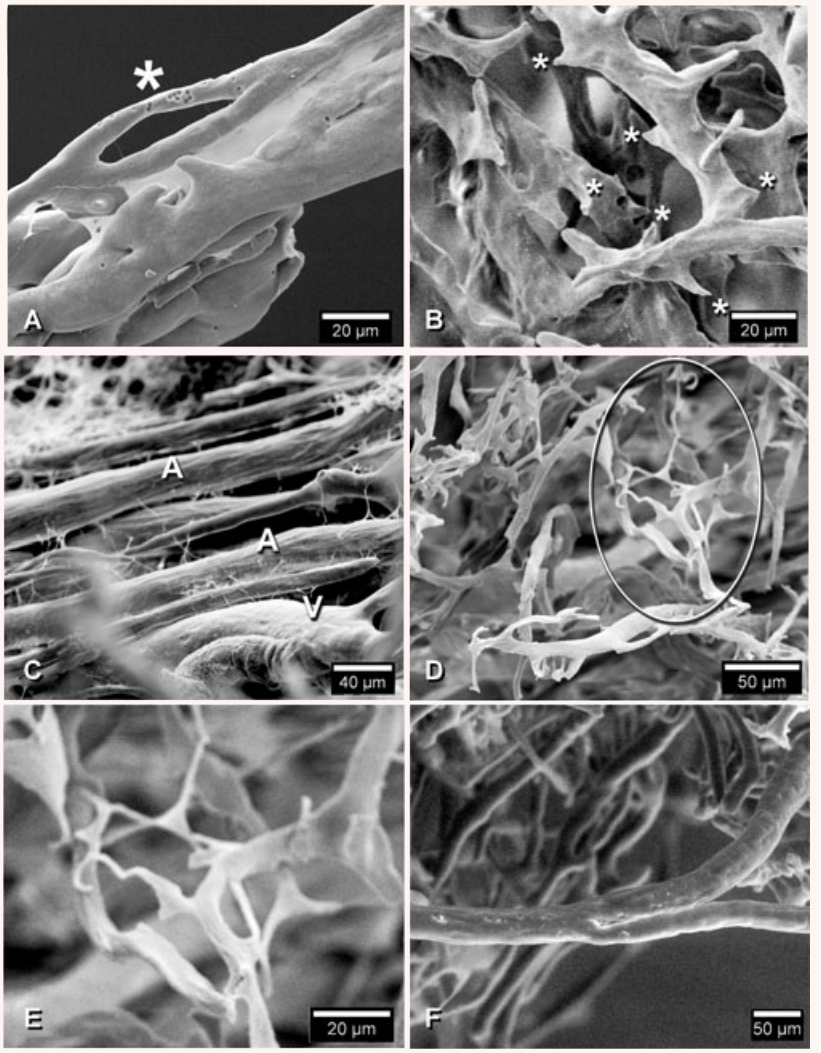

Fig. 6 (**A**) (SEM, 2 weeks) Capillary loop formation *via* IAR is accomplished by division of a nascent vascular conduit into two parallel ones. This process offers an energy saving alternative for optimalization of a vascular system. (**B**) (SEM, 2 weeks) Forward sprouting angiogenesis in a angiogenic 'hot spot'. Asterisks represent neovascular sprouts. (**C**) (SEM, 8 weeks). The arterial or venous character of a vessel can be identified by the shape of the nuclear imprints on the cast. Long spindle-shaped endothelial nuclei are indicative for artery (A); rounded and planar nuclear imprints indicate a vein (V). Here, vessels demonstrate an arterial or venous character in the 8-week replica. (**D**) (SEM, 4 weeks) Formation of intercapillary loops and detail (**E**). New lumina are generated between capillaries to serve as interconnection, where none exist. (**F**) (SEM, 4 weeks). IBR is a means of optimizing the branching in terms of branching angle and interbranching distance. Interstitial pillars form along the long axis of the vessels prior to the branching point.

membrane model) the propagation of an angiogenic front has been assessed over time in terms of a distance covered from starting point with similar proliferation assays existing for corneal models, as well. For evaluation of *in vivo* experiments related to questions of vasculoangiogenesis or antiangiogenesis, measurements by way of histomorphometry, angiography after injection of contrast medium, as well as quantitative methods of molecular biology have also been applied. While RT–PCR quantitative analysis can provide information in one dimension (time), histology offers a two-dimensional understanding on the plane of the specimen under inquiry. Three-dimensional clues must be extrapolated into space and time, by combining information of several such sections [26]. Finally, corrosion casting has been very valuable in elucidating some stereomorphological aspects of angiogenesis; however, relationships to the surrounding tissues are difficult to decipher. High-resolution tomography by means of micro CT or magnetic resonance imaging, are likely to bring about a new era in research of early neovascularization.

At later stages, however, evaluation becomes somewhat more complex. From a physiological point of view, during the phase of remodelling in addition to vasculogenesis and angiogenesis, arteriogenesis is also involved. As the process of maturation for a given neovascular network is basically a process of metamorphosis, it is difficult to describe changes of form, in times when everything in research has to be appraised in numbers and statistics. Finally, the consequences drawn by determining the degree of maturation have still to be defined. Before we look into ways to influence this process extrinsically, we have to determine the profit gained from enhancing or antagonizing it. After all, it should be emphasized, that at later stages of microvascular network development, the density and calibre of vessels is dictated by perfusion demands of the tissue, as well as local haemodynamic attributes.

Involution of the vessel as a unit is important for evolution of the network as a whole. Under this assumption, ongoing neovascularization with a decrease of vascular density over time does not present a paradox—a network gets rid of its superfluous branches to optimize itself and save energy.

This notion is reflected by the findings in this study. Initially, between week 2 and 4 the number of capillaries in the ROI increased in all segments concomitant to a process of early angiogenesis characterized by proliferation of endothelial cells and expansion of the nascent capillaries. The number of capillaries at the non-arterial segments was significantly higher than at the artery, confirming the knowledge that new vessels emerge from the venous side of the circulation [19]. A rise in cross-sectional area of lumina as % FA *versus* total area within ROI was an indicator of increased perfusion capacity. A higher perfusion capacity was accomplished by a higher number of vessels. At later stages, after week 4, the findings were different: An additional rise in the % FA was accompanied by a decrease in the absolute number of vessels, an observation demonstrating that the existing or remaining vessels increased in diameter to accommodate increased perfusion. During this process the decrease in number of capillaries by means of involution of superfluous conduits and 'pruning' (regression) left some of the vascular elements forced to persist and enlarge into afferent arterioles or efferent venules (persistence). This whole process resulted in a perfusion system accommodating vessels of different orders, from arterioles, precapillary arterioles, capillaries and postcapillary venules, to draining venules and veins. The assumption that the variance of calibre is a parameter connected to maturity of a vascular network has been herein suggested and could be used similarly in the future.

The presence of capillary loops cannot be displayed by histology. Three-dimensional illustration of the vascular bed can be performed by electron microscopy of corrosion casts. In this experimental setting, presence of capillary loops was verified in all specimens placing this phenomenon in the early stages of vascular remodelling. Both the processes of intercapillary interconnection (Fig. 6D and E) as well as intussusception (Fig. 6A) were observed. Assignment of the vessels into arterial or venous circulation commenced after week 4, after feeding vessels had been established (Fig. 6C).

PCT and SMC were visualized as early as 2 weeks after implantation of the AV loop. Traditionally, pericytic migration is thought to follow endohelial cell (EC) proliferation to provide for stability of the new capillary, precipitate inactivation of the ECs and bring angiogenesis to a halt. However, in a recent work, proliferation of PCs was shown to precede proliferation of ECs. Longitudinal formations void of a lumen that stained for both lectin as well as α-SMA might reflect this very theory [13].

In this setting, albeit the investigation took place within the frame of an *in vivo* experiment, the construct represented a closed system in an isolation chamber. The use of a porous biogenic hardmatrix ensured a constant circular geometry of the AV loop as vascular axis served as geometry. Furthermore, inflammatory components of angiogenesis could be grossly circumvented as postulated before by the authors [22]. All in all, in this study we were able to confirm processes of regression in a bioartificial construct and place them in a time frame within the first 2 months. Additionally, variance of calibre was proposed as a parameter of maturity in a vascular assembly and other morphologic phenomena of remodelling were visualized by corrosion casting and discussed critically. Better insight into mechanisms of vascular remodelling will see us through translating the experimental knowledge gained on angiogenesis into therapeutic benefits.

Acknowledgements

This study was supported by grants from Xue-Hong and Hans Georg Geis, University of Erlangen ELAN Fonds, as well as Tutogen Medical Inc. We wish to thank Ms. Ilse Arnold for her help with immunohistology and Mr. Peter Reinhardt for preparation of the isolation chambers.

References

1. **Greene HSN.** Heterologous transplantation of mammalian tumours. *Exp Med.* 1941; 73: 461–74.
2. **Folkman J.** Tumor angiogenesis: therapeutic implications. *N Engl J Med.* 1971; 285: 1182–6.
3. **Li VW, Li WW.** Antiangiogenesis in the treatment of skin cancer. *J Drugs Dermatol.* 2008; 7: s17–24.
4. **Petersen I.** Antiangiogenesis, anti-VEGF(R) and outlook. *Recent Results Cancer Res.* 2007; 176: 189–99.
5. **Bleiziffer O, Eriksson E, Yao F, *et al.*** Gene transfer strategies in tissue engineering. *J Cell Mol Med.* 2007; 11: 206–23.
6. **Zavan B, Abatangelo G, Mazzoleni F, *et al.*** New 3D hyaluronan-based scaffold for *in vitro* reconstruction of the rat sciatic nerve. *Neurol Res.* 2008; 30: 190–6.
7. **Horch RE, Pepescu LM, Vacanti C, *et al.*** Ethical issues in cellular and molecular medicine and tissue engineering. *J Cell Mol Med.* 2008; 12: 1785–93.
8. **Polykandriotis E, Arkudas A, Horch RE, *et al.*** Autonomously vascularized cellular constructs in tissue engineering: opening a new perspective for biomedical science. *J Cell Mol Med.* 2007; 11: 6–20.
9. **Fiegel HC, Kaufmann PM, Bruns H, *et al.*** Hepatic tissue engineering: from transplantation to customized cell-based liver directed therapies from the laboratory. *J Cell Mol Med.* 2008; 12: 56–66.
10. **Arkudas A, Tjiawi J, Saumweber A, *et al.*** Evaluation of blood vessel ingrowth in fibrin gel subject to type and concentration of growth factors. *J Cell Mol Med.* 2009; 13: 2864–74.
11. **Kurz H.** Physiology of angiogenesis. *J Neurooncol.* 2000; 50: 17–35.
12. **Hanahan D.** Signaling vascular morphogenesis and maintenance. *Science.* 1997; 277: 48–50.
13. **Virgintino D, Ozerdem U, Girolamo F, *et al.*** Reversal of cellular roles in angiogenesis:

implications for anti-angiogenic therapy. *J Vasc Res.* 2008; 45: 129–31.

14. **Nehls V, Denzer K, Drenckhahn D.** Pericyte involvement in capillary sprouting during angiogenesis *in situ*. *Cell Tissue Res.* 1992; 270: 469–74.
15. **Shin D, Garcia-Cardena G, Hayashi S, *et al.*** Expression of ephrinB2 identifies a stable genetic difference between arterial and venous vascular smooth muscle as well as endothelial cells, and marks subsets of microvessels at sites of adult neovascularization. *Dev Biol.* 2001; 230: 139–50.
16. **Gale NW, Baluk P, Pan L, *et al.*** Ephrin-B2 selectively marks arterial vessels and neovascularization sites in the adult, with expression in both endothelial and smooth-muscle cells. *Dev Biol.* 2001; 230: 151–60.
17. **Yancopoulos GD, Klagsbrun M, Folkman J.** Vasculogenesis, angiogenesis, and growth factors: ephrins enter the fray at the border. *Cell.* 1998; 93: 661–4.
18. **Djonov VG, Kurz H, Burri PH.** Optimality in the developing vascular system: branching remodeling by means of intussusception as an efficient adaptation mechanism. *Dev Dyn.* 2002; 224: 391–402.
19. **Diaz-Flores L, Gutierrez R, Varela H.** Angiogenesis: an update. *Histol Histopathol.* 1994; 9: 807–43.
20. **Lametschwandtner A, Minnich B, Kachlik D, *et al.*** Three-dimensional arrangement of the vasa vasorum in explanted segments of the aged human great saphenous vein: scanning electron microscopy and three-dimensional morphometry of vascular corrosion casts. *Anat Rec A Discov Mol Cell Evol Biol.* 2004; 281: 1372–82.
21. **Kneser U, Polykandriotis E, Ohnolz J, *et al.*** Engineering of vascularized transplantable bone tissues: induction of axial vascularization in an osteoconductive matrix using an arteriovenous loop. *Tissue Eng.* 2006; 12: 1721–31.
22. **Polykandriotis E, Horch RE, Arkudas A, *et al.*** Intrinsic *versus* extrinsic vascularization in tissue engineering. *Adv Exp Med Biol.* 2006; 585: 311–26.
23. **Polykandriotis E, Tjiawi J, Euler S, *et al.*** The venous graft as an effector of early angiogenesis in a fibrin matrix. *Microvasc Res.* 2008; 75: 25–33.
24. **Lametschwandtner A, Lametschwandtner U, Weiger T.** Scanning electron microscopy of vascular corrosion casts—technique and applications. *Scan Electron Microsc.* 1984: 663–95.
25. **Mukai N, Akahori T, Komaki M, *et al.*** A comparison of the tube forming potentials of early and late endothelial progenitor cells. *Exp Cell Res.* 2008; 314: 430–40.
26. **Sokolis DP.** Passive mechanical properties and constitutive modeling of blood vessels in relation to microstructure. *Med Biol Eng Comput.* 2008; 46: 1187–99.